Transparency and long-ranged fluctuations: The case of glass ceramics

M. Mattarelli, G. Gasperi, M. Montagna, and P. Verrocchio
Dipartimento di Fisica, Universitá di Trento, Via Sommarive 14, I-38100 Trento, Italy
(Received 18 July 2010; published 29 September 2010)

Glass ceramics with nanosized crystallites shows an unexpected high transparency, which is not accounted for by the Rayleigh theory of light scattering. Simple analytic arguments ascribe this large transparency to large spatial correlations in the number distribution of the nanocrystallites. Introducing a two-dimensional lattice model that mimics the nucleation and the coarsening phenomena leading to their formation, we show that the extent of such correlations is determined by the spatially limited diffusion of the particles that form the crystallites.

DOI: 10.1103/PhysRevB.82.094204 PACS number(s): 78.20.Bh, 61.05.cf, 78.35.+c, 81.05.Pj

I. INTRODUCTION

Glass ceramic are composite materials formed by a glass matrix containing nanometer-sized crystals. Their structure makes them valuable for application in photonics as they combine the spectroscopic properties of crystals with the mechanical properties of glasses.[1–5] Nanoglass ceramics are usually built via a thermal treatment of a multicomponent glass.

A strong optical scattering, which is highly detrimental for applications, would be expected for these systems due to difference of the refractive index between the nanocrystals and the amorphous matrix where they are embedded. Yet, many glass ceramics exhibit a transparency that is orders of magnitude higher than the predictions of Rayleigh theory, which assume a collection of random scatterers with no spatial correlation. This property of nanoglass ceramics has been termed ultratransparency[1–6] and seems to be related to large spatial correlations, which would be responsible for the constructive interference of the scattered field, as it was first suggested by Tick.[2] The spatial correlation (and the interference) are described by the static structure factor $S(q)$.[6–10] Different mechanisms have been proposed to explain such spatial correlations. On one hand Hopper,[8] and then Hendy,[9] have considered the effects due to a spinodal decomposition which induces a homogeneity for length scale larger than some spinodal distances. On the other hand, Shepilov[7] has studied the effects of the short range correlation induced by the processes of nucleation and growth of the nanocrystals, which prevents the formation of contacting particles as expected for a completely random distribution. In the work of Edgar,[11] the homogeneity is obtained at even shorter distance, considering that nucleation creates a core-shell structure where the average refractive index is conserved.

In a previous work, by computing the $S(q)$ of a system of equal particles created via random sequential addition (RSA),[10,12] which can be thought as a simple model system of nanoglass ceramics, it has been shown that a correlation between the nanocrystals certainly arises due to their finite sizes and that this yields a significant increase in transparency although not enough to explain the ultratransparency which is observed in experiments. The model was extended in order to include a size distribution of the nanocrystals.[13] Thus it has been postulated that the crucial quantity in determining the ultratransparency is the density fluctuation of scatterers on larger scales than the wavelength of incident light. The attenuation is proportional to this fluctuation that can be much lower than that obtained from Poisson distribution for fully random distributed particles. Moreover, it was suggested that the process of aggregation by thermal diffusion produces low-density fluctuations at long range. As a matter of fact, the growth of the crystallites proceeds by coarsening even when practically the whole content of the instable component is already precipitated in the crystalline phase due to the coalescence of small crystallites into larger ones. Thus, the particle density and its fluctuations (as well as the average and the variance in the distribution of crystallite sizes) will change during the thermal annealing. A crucial role will then be played by the diffusion length, ξ, i.e., the average distance covered by a particle during the annealing. On general ground, one expects that a strong correlation in the density fluctuations is introduced by the annealing procedure. In particular, over length scales R larger than ξ the fluctuations are smaller than those at shorter distances. As a matter of fact, if the nanocrystallites grow mostly out of the material collected in a basin of size ξ, the number of building blocks and then of nanoparticles in a much larger volume will have relative fluctuations similar to those of the parent glass. Then, according to the above framework a decrease in the intensity of the scattered light is due to the decrease of the relative fluctuations in the number of scatterers at length scales larger than ξ. In order to confirm such scenario, in the present work we first discuss a simple argument to relate ultratransparency and density fluctuations (Sec. II), then we study a simplified bidimensional model of diffusing particles (the building blocks of nanocrystallites) which have also a certain probability to aggregate and form large clusters (the nanocrystallites) (Sec. III).

II. THEORY

When the light is scattered by a macroscopic system of N equal scattering centers of nanometric size (i.e., in the regime $d \ll \lambda$, where d is the size of the particle and λ is the wavelength of the incident radiation), the total cross section σ is related to the structure factor $S(q)$ of the system by the relation

$$\sigma = N \int d\Omega S(q) \left[\frac{\partial \sigma_{\mathrm{Ray}}}{\partial \Omega} \right], \tag{1}$$

where $\partial\sigma_{\mathrm{Ray}}/\partial\Omega$ is the differential cross section for the Rayleigh scattering of a single particle, q is the exchanged momentum $2(2\pi/\lambda)n \sin(\theta/2)$, n is the refraction index, and θ the scattering angle.[14] When λ is far larger than any characteristic length scale within the system the contribute to the cross section in Eq. (1) comes from the very low-q tail of $S(q)$. In absence of correlations among the particles, one should expect that $S(q\sim 0)\sim 1$ and $\sigma \sim N\sigma_{\mathrm{Ray}}$ (where σ_{Ray} is the integrated cross section). It turns out to be useful to characterize the structure factor in terms of the relative variance $\Delta(R) \equiv (\langle N(R)^2\rangle - \langle N(R)\rangle^2)/\langle N(R)\rangle$ of the number of scatterers $N(R)$ within a sphere of radius R. We note that $\Delta(R\to\infty)\to 0$. Structure factor and $\Delta(R)$ are related by[15]

$$S(q) - 1 = \int_0^\infty dR \frac{\sin qR}{qR} \frac{d\Delta(R)}{dR}. \tag{2}$$

The uncorrelated case corresponds to $\Delta(R)=1$ (Poisson distribution) and $S(q)=1$. Within this approach, the effect of the limited diffusion during the thermal annealing can be introduced by making the rough approximation

$$\Delta(R) \sim \begin{cases} 1 & R < \xi \\ 0 & R > \xi, \end{cases} \tag{3}$$

which is meant to describe the fact that for $R<\xi$ the diffusion decorrelates totally the position of the particles. Within this approximation we may approximate in the integral

$$\frac{d\Delta(R)}{dR} \sim -\delta(R-\xi) \tag{4}$$

obtaining

$$S(q) = 1 - \frac{\sin q\xi}{q\xi} \to_{q\to 0} (q\xi)^2/6. \tag{5}$$

In this limit, the cross section in Eq. (1) becomes

$$\sigma = N \frac{\sigma_{\mathrm{Ray}}}{3} \left(\frac{2\pi\xi n}{\lambda} \right)^2, \tag{6}$$

which accounts for an increasing of the transparency of a few decades when the ratio ξ/λ is small enough. For realistic systems the assumption in Eq. (3) is a very drastic one, since the fluctuations of $N(R)$ decay in a much smoother way for $R>\xi$.

III. NUMERICAL SIMULATION

In order to move beyond the drastic approximation of Eq. (4), we introduce a simple lattice model of diffusion-limited crystal growth,[16] whose dynamical rule aims at mimicking the formation of nanocrystallites out of a glass system. Fixing the filling factor φ, we place φM^2 building blocks on a square grating (with lattice spacing d) of size $M\times M$ with periodic boundary conditions (here we focus on the case $\varphi = 0.25$). The starting configurations can be random or spatially periodic (square lattice). By calling $n_i^{(r)}$ the number of rth neighbors to the site i, a dynamics of the model is introduced by choosing the probability p_{ij} for a given block to move from the site i to the site j at each time step. In our case, we have

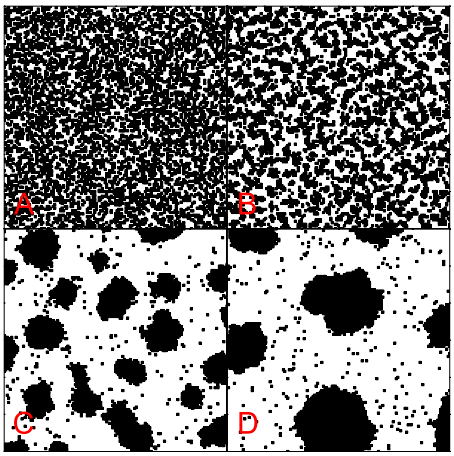

FIG. 1. (Color online) The time evolution (starting from a random distribution, A) according to the dynamics in Eq. (7). The system at times $t=1\times 10^2$ (B), 1×10^4 (C), and 2×10^6 (D) is shown.

$$p_{ij} = \left(1 - \frac{n_i^{(1)}}{8}\right)^c \left\{ p_s \left[\frac{1 + u(n_j^{(1)} + 0.5 n_j^{(2)})}{\sum_j 1 + u(n_j^{(1)} + 0.5 n_j^{(2)})} \right] \right\} \tag{7}$$

(we take the parameters $c=4$, $p_s=1/2$ and $u=0.3$). Roughly speaking, the first multiplicative factor controls the rate of evaporation of clusters. When $c>1$ small clusters evaporate much faster than the largest ones. The second one, on the other hand, simply tends to make such clusters more compact and smooth. In Fig. 1 we show the time evolution of a system with $M=2048$ up to 2×10^6 time steps. We show that such evolution corresponds mostly to the formation of round clusters of larger and larger size.

We will consider that this collection of scattering units diffuse the light with an efficiency which is independent on the actual configuration. In other words, each building block, which will aggregate into particles, has a constant polarizability and any induced effect is neglected. In this case the intensity of the scattered electric field becomes proportional to the static structure factor of the building blocks.

$$S(q) = \frac{\left| \sum_i \exp(i\mathbf{q}\mathbf{r}_i) \right|^2}{\varphi M^2}, \tag{8}$$

where the sum runs on the positions $\mathbf{r}_i$ of the building blocks.

IV. RESULTS AND DISCUSSION

Figure 2 shows the time evolution of $S(q)$ in the case of (a) periodic and (b) random initial conditions. At $t=0$, the structure factor of the spatially periodic system shows only Bragg peaks, while that of the random system is a constant at

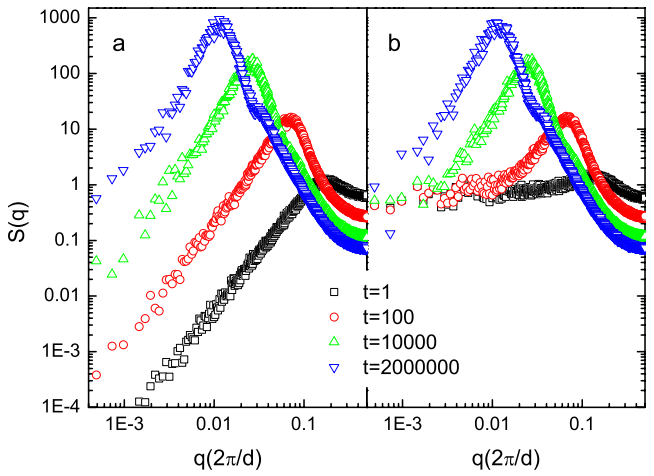

FIG. 2. (Color online) $S(q)$ for the systems obtained by the diffusion model starting from (a) a square lattice and (b) a random configuration, at four representative times.

about 0.75 (consistently with $\varphi=0.25$). After a few time steps the $S(q)$ of the two systems becomes equivalent in the high q region, down to the first diffraction peak. Such peak shifts with time to lower and lower q, as the mean size and distance among particles increases. On the other hand, in the small q region, the $S(q)$ of the two samples is different for short times and tends to become similar only at large enough times. More quantitatively, the two curves were fitted by the general low-q behavior, $S(q)=S_0+b^2q^2$. The results of the fit are shown in Fig. 3. The parameter S_0 remains initially constant respectively at values $S_0=0$ and $S_0=0.75$ for the crystalline and disordered initial systems and in both cases eventually saturates at a very small value (0 within the error bars). Thus we are very close to the limit of Eq. (4). More importantly, the parameter b, which is related to the typical length ξ [see Eq. (5)], in both cases increases proportionally to the diffusion length

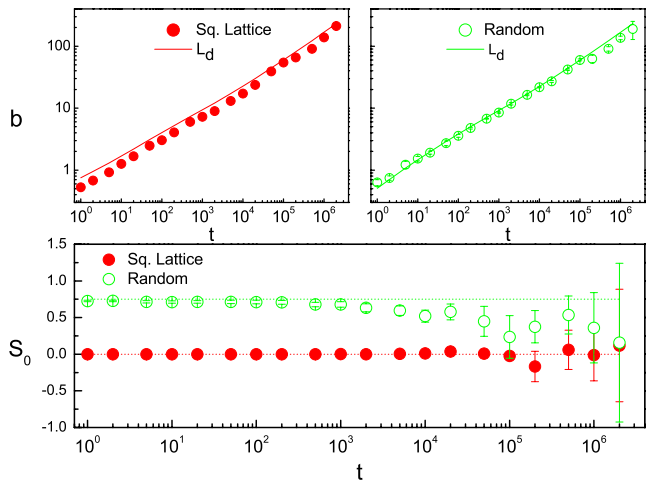

FIG. 3. (Color online) Values of the parameters obtained by fitting the low-q tail of $S(q)$, at different times, by $S(q)=a+b^2q^2$ for the two starting systems: square lattice (dots) and random (circles). The solid lines in the upper graphs show the calculated diffusion lengths.

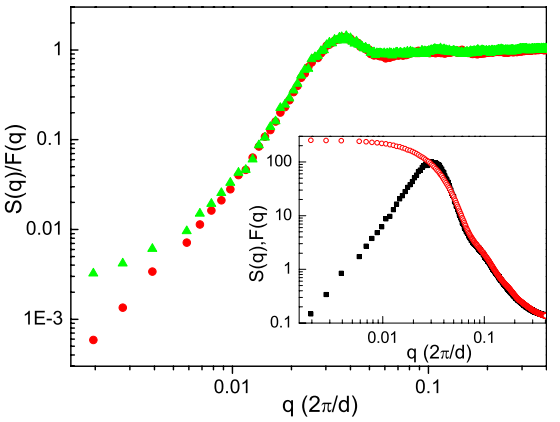

FIG. 4. (Color online) Particle to particle interference effects, measured as the ratio between the actual scattered intensity, and that in the absence of interference (see text), calculated at $t=50\,000$ for square lattice (squares) and random (triangles) initial configurations. The inset shows the two quantities, whose ratio is presented in the figure: $S(q)$ of the building blocks, i.e., the true scattered intensity (squares) and that given by Eq. (8) (circles), for the crystalline initial condition.

$$L_d = \frac{1}{\varphi M^2}\sum_i [\mathbf{r}_i(t) - \mathbf{r}_i(0)]^2. \tag{9}$$

We claim then that the length ξ, which controls the number fluctuations, coincide with the diffusion length L_d, which has to be ascribed only to the dynamic process.

Summarizing, the transparency of the glass ceramics remains that of the parent glass in the first steps of growth and coarsening and begins to be reduced when $\xi^2 q_{\max}^2 = (\frac{4\pi}{\lambda} n\xi)^2$ becomes comparable with S_0. Note that the $(\xi/\lambda)^2$ dependence is consistent with the result of Eq. (6). Besides the possible explanation of the observed ultratransparency in glass ceramics, from the above analysis it turns out that the diffusion length ξ appears in the q^2 term of the $S(q)$. This suggest that ξ can be inferred by the measure of the structure factor in the very low-q range in light or small-angle x-ray scattering (SAXS) experiments. We note that the structure factor alone (Fig. 2) do not clarify to which extent the Rayleigh scattering intensity is reduced by interference effects since the $S(q)$ is obtained by adding all the contributions from the single building blocks. Thus, in order to emphasize the role played by interference, we define the quantity

$$F(q) = \frac{\sum_j \left|\sum_i \exp(i\mathbf{q}\mathbf{r}_i)\right|^2}{N}, \tag{10}$$

where the index j runs on the N clusters and the index i runs on the building blocks of the jth cluster. $F(q)$ is then proportional to the scattered intensity in absence of any interference of fields from different clusters. The $F(q)$, $S(q)$ and their ratio are compared in Fig. 4 for $t=50\,000$. We see that, at low q, $F(q)\simeq$const. Such comparison suggests that the interference among different clusters is negligible for q higher than q_{peak}, weakly constructive at $q\sim q_{peak}$, and strongly

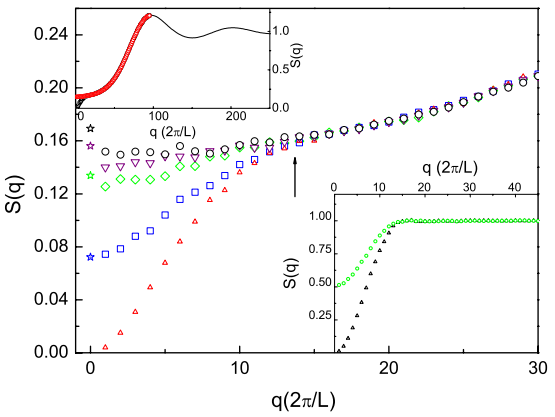

FIG. 5. (Color online) Main panel: $S(q)$ at small q's for a modified RSA system (see text), with m_1 particles in each of 16 cubic sub-boxes of size l, and $m_2 \times 16$ particles, with $m_2 = 100 - m_1$, randomly in the whole box. Circles: $m_1 = 0$; inverted triangles: $m_1 = 50$; diamonds: $m_1 = 70$; squares: $m_1 = 90$; and triangles: $m_1 = 100$. The arrow indicates $q = 2\pi/l$. The stars, placed at $q = 0$, are obtained from the distribution of the number of particles in the 16 boxes, and correspond to the quantity $\sigma^2/100$. Left, top: $S(q)$ in a more extended range for the limiting cases $m_1 = 0$ (circles) and $m_1 = 100$ (triangles). $S(q)$ is almost independent of m_1 for $q > 2\pi/l$. The solid line shows $S(q)$ calculated from the $g(r)$ and is common to all m_1 within the thickness of the line. Right, bottom: $S(q)$ for the case $\varphi = 0$, $m_1 = 100$ (triangles) and $m_1 = 50$ (circles).

destructive in the low-q range. For light scattering, the $0 < q < q_{\max} = \frac{4\pi}{\lambda} n$ is the important range.

Finally, in order to confirm that at small q's the structure factor decreases as the particles become more correlated on larger scales than ξ, we introduce a modified RSA model,[10,12] where both ξ and the number fluctuations on that length scale are fixed *a priori*. As a matter of fact, in our modified RSA, the box containing N equal spherical particles is divided in n equal cubic sub-boxes of size l (which now plays the role of ξ), each containing on average $m = N/n$ particles. While in the original RSA model, the N particles are placed at random in the box, the only constraint being that they cannot superimpose, within our modified RSA model we sequentially place m_1 particles in each of the n sub-boxes, and finally $m_2 \times n$ particles, with $m_2 = m - m_1$, randomly in the whole box. The constraint that particles cannot superimpose is maintained (with $m_1 = 0$, $m_2 = m$ standard RSA is recovered). The relative variance of the number distribution for the sub-boxes σ^2/m (see Fig. 5) decreases as m_1 increases and becomes zero for $m_1 = m$. Figure 5 shows the $S(q)$ for $m_1 = 0$, 50, 70, 90, 100, and $m = 100$, at $\varphi = 0.2$. The box has 16 cubic sub-boxes, of size l, along a line with a volume $V = L \times l \times l$ ($L = 16 \times l$, $N = 1600$). We check that $S(q)$ does not depend on the shape by comparing with the cubic box case ($4 \times 4 \times 4 = 64$ sub-boxes, $N = 6400$, $m = 100$, and $V = 64 \times l^3$). We note that $S(q)$ depends on m_1 only in the very low-q range. Figure 5 (top, left) shows $S(q)$ in a more extended range for the two extreme cases of $m_1 = 0$ and $m_1 = m$. For high-q values, this calculation was done from the pair correlation function, $g(r)$, a faster method which avoids the wide fluctuations of the $S(q)$ calculated by Eq. (1), but fails in reproducing the low-q tail.

In order to disentangle the effects of the RSA, which, simply avoiding particle superposition, in fact produces correlations at any distance, from the effect of a defined long-range density fluctuation, we have done the some calculation on samples with $\varphi = 0$. In this case, the RSA constraints are no more active and the particles can be placed at any small distance. Again, a fraction of particles (m_1/m) are equally placed in the n sub-boxes and a part is placed randomly in the whole volume. Figure 5 (right, bottom) shows the result of the calculation for $m_1 = 50$ and $m_1 = 100$. When the density fluctuations are decreased by increasing m_1, a crossover from $S(q) = 1$ to a new low-q tail appears approximately at $q = 2\pi/l$. The curve has a low-q limit, S_0, given by $S_0 = m_2/m = (1 - m_1)/m$. In this case, unlike what we find for $\varphi = 0.2$, the (relative) density fluctuations remain the same $(\sigma^2/m = m_2/m)$ at any distance higher than the size of the sub-boxes. Weak oscillations with maxima at multiples of $q \simeq 2\pi/l$ appear in $S(q)$. The main result shown by Fig. 5 is the presence of a crossover at $q \simeq 2\pi/l$ from a nearly constant behavior, $S(q) = S_0 + Aq^2$, in the absence of the constraint, to a new parabolic curve, $S(q) = S_0' + A'q^2$, with $S_0' < S_0$ and $A' > A$.

V. CONCLUSIONS

We have shown that the existence of a characteristic length ξ over which density fluctuations are much smaller with respect to the Poisson case may explain the phenomenon of ultratransparency in the visible domain for glass ceramics, a class of materials of great interest for nanophotonics. This length ξ is related to the limited diffusion in the growth process of the crystallites. Moreover the effects of correlations over different length scales may be disentangled. The high-q range depends on the microscopical arrangement as particle structure and small range distance while the low q range only on the long-range density fluctuations, related to the diffusion length. Finally, the diffusion length ξ might be inferred by means of light scattering or SAXS experiments, in the low-q tail of $S(q)$.

ACKNOWLEDGMENTS

P.V. has been partly supported under Research Contracts No. FIS2009-12648-C03-01 and No. FIS2008-01323 by MICINN, Spain.

[1] Y. Wang and J. Ohwaki, Appl. Phys. Lett. **63**, 3268 (1993).
[2] P. A. Tick, N. F. Borrelli, L. K. Cornelius, and M. A. Newhouse, J. Appl. Phys. **78**, 6367 (1995).
[3] V. K. Tikhomirov, D. Furniss, A. B. Seddon, I. M. Reaney, M. Beggiora, M. Ferrari, M. Montagna, and R. Rolli, Appl. Phys. Lett. **81**, 1937 (2002).
[4] M. C. Gonçalves, L. F. Santos, and R. M. Almeida, C. R. Chim. **5**, 845 (2002).
[5] M. Mortier, A. Monteville, G. Patriarche, G. Mazé, and F. Auzel, Opt. Mater. **16**, 255 (2001).
[6] A. Edgar, G. V. M. Williams, and J. Hamelin, Curr. Appl. Phys. **6**, 355 (2006).
[7] M. P. Shepilov, A. E. Kalumykov, and G. A. Sycheva, Phys. Chem. Glasses-B **47**, 339 (2006).
[8] R. W. Hopper, J. Non-Cryst. Solids **70**, 111 (1985).
[9] S. Hendy, Appl. Phys. Lett. **81**, 1171 (2002).
[10] M. Mattarelli, M. Montagna, and P. Verrocchio, Appl. Phys. Lett. **91**, 061911 (2007).
[11] A. Edgar, Appl. Phys. Lett. **89**, 041909 (2006).
[12] S. Torquato, O. U. Uche, and F. H. Stillinger, Phys. Rev. E **74**, 061308 (2006).
[13] M. Mattarelli, M. Montagna, and P. Verrocchio, Philos. Mag. **88**, 4125 (2008).
[14] H. C. van de Hulst, *Light Scattering by Small Particles* (Dover, New York, 1981).
[15] J. P. Hansen and I. R. McDonald, *Theory of Simple Liquids* (Academic Press, London, 1990).
[16] Y. Saito, *Statistical Physics of Crystal Growth* (Word Scientific, 1996).